Nonlinear Dynamics (2006)
DOI: 10.1007s11071-005-9007-7

Multidimensional Damage Identification Based on Phase Space Warping: An Experimental Study

DAVID CHELIDZE* and MING LIU
Department of Mechanical Engineering and Applied Mechanics, University of Rhode Island, Kingston, RI 02881, USA;
**Author for correspondence (e-mail: chelidze@egr.uri.edu)*

(Received: 19 January 2005; accepted: 25 October 2005)

Abstract. A multidimensional damage identification scheme developed in previous work is modified and investigated experimentally. An experimental apparatus consists of a driven two-well magneto-elastic oscillator, where a cantilever beam vibrates in a magnetic potential field perturbed by two electromagnets. These electromagnets are activated by a computer controlled power supply and their terminal voltages are considered a two-dimensional damage variable. The effect of total change in the supply voltage of the electromagnets is approximately 4% shift in the experimentally measured natural frequencies of small oscillations in each well of the potential. Experimental runs are started in a nominally chaotic regime. The battery voltages are altered on specific trajectories in the damage (voltage) phase space. Damage identification is accomplished based on the elastic vibration data collected using laser vibrometers and a accelerometer. The phase space warping based damage tracking feature vectors are estimated using a new phase space partitioning scheme. The damage identification is achieved by applying smooth orthogonal decomposition to the obtained statistics. The effect of the data record size on the quality of reconstructed damage trajectory is investigated in a series of experiments. It is also demonstrated that the new partitioning scheme considerably improves signal-to-noise ration of the identified damage states.

Key words: dynamical systems, diagnostics, condition monitoring, health monitoring, phase space reconstruction, multidimensional damage identification

1. Introduction

In engineering systems, gradual component deterioration leads to imminent failure. High demands for safety and reliability stimulate critical interest in developing damage diagnosis technology. However, complexity of modern systems makes such diagnosis hard, especially when several damage mechanisms are simultaneously present in a system. A wide variety of solutions are proposed in existing literature, however most of them focus on diagnosis of some special scalar damage processes. Currently, the majority of proposed solutions for multi-dimensional damage diagnosis are based on model updating methods [2, 15, 18, 22], for which an accurate analytical model of the system *is necessary*. In previous work, a multidimensional damage identification method [5] has been developed based on *phase space warping* (PSW) concept [4]. This method uses a dynamical systems perspective and *does not* require the knowledge on the analytical model of the system. The utility of this approach was tested using numerical experiments and analytical models. Here, a modified version of the method is presented and tested in experiments. The method is modified by employing a new phase space partitioning scheme that allows for improved accuracy of damage identification results. In experiments both the effects of changing data record size and sensitivity to different sensing solutions are investigated.

In the next section, a brief literature survey is provided to outline the current state-of-the-art in damage identification utilizing systems' nonlinear properties. A brief description of the old damage identification

technique is also provided for completeness, with a new phase space partitioning component. Then an experimental system is described, and the damage identification is applied to the collected data from two different sensors. This is followed by the discussion of results and conclusions.

2. Background

There is a large body of literature related to damage identification. Important review articles are from Doebling et al. [10, 11], and its updated version from Sohn et al. [23]. Several other reviews focus on more specific fields, e.g., Zou et al. [29] focus on vibration based model-dependent SHM for composite structures; Edwards et al. [12] review damage diagnosis techniques for rotating machinery; and Zhou and Sim [28] provide a review for fibre optic damage detection and assessment systems embedded in fibre-reinforced composite structures. In [4, 5] a general discussion of available literature is also provided and interested reader is referred to these papers for further information. Here, we review some new developments in damage identification based on nonlinear dynamics methods.

It is generally understood that the damage accumulation causes structural changes in a system that lead to bifurcations, loss of stability, and catastrophic failures at the end. For example, Foong et al. [14] investigate dynamical behavior of a beam due to a propagating fatigue crack. They demonstrate that for a stationary harmonic excitation, the vibration of the beam changes from periodic to chaotic with the propagation of the crack through bifurcation. Thus, the appearance of nonlinear phenomenon in a nominally linear systems can be used as an indication of damage. Douglas et al. [1] propose a damage identification approach based on model deduction near bifurcations. This method uses an assumption that an undamaged system is linear, and nonlinearity is only introduced by damage.

Some nonlinear measures are investigated by Wang et al. [27] for practical damage detection, and correlation dimension's ability to provide some intrinsic information about an underlying dynamical system is used to classify different faults. Hively and Protopopescu [16] study system dynamics in a reconstructed phase space which is divided into several small bins and damage detection is achieved using a phase-space dissimilarity measures. This is also shown to be more stable, compared with methods using traditional nonlinear measures such as Lyapunov exponents, Kolmogorov entropy, and correlation dimension.

The benefits of working in a phase space of chaotic system are utilized by Nichols, Todd, Virgin and coauthors by exciting a nominally linear systems using chaotic signals. In this way one works with broadband signals that are low-dimensional, deterministic, and exhibit sensitivity to small changes in system parameters. A series of related methods [19, 25, 26] are applied to detect loss of preload in a bolted joint on a frame structures.

Almost all these methods are based on extracting long-term invariant features from measured time series to detect damage. However, systems with damage accumulation are usually structurally unstable—drifting system parameters cause bifurcations in steady state behavior. Therefore, long-term invariant features are not expected to be a smooth functions of drifting parameters and are unsuitable for continuous damage tracking.

In previous work [4, 5, 6, 9], a novel damage identification and diagnosis method has been developed in a dynamical system framework [8]. In this work, one-to-one relationship between PSW-based tracking vectors and actual damage states has been demonstrated. This approach has been successfully applied to one-dimensional damage identification problem [4, 6]. By introducing new feature vectors, and *smooth orthogonal decomposition* (SOD) [5], the method has been extended to address a multi-dimensional damage identification problem.

3. A Brief Outline of Damage Identification Method

Based on dynamical system approach [8], damage is regarded as a slow-time state variable evolving in a hierarchical dynamical system, where a fast-time system dynamics is coupled to a slow-time damage evolution. We assume that we can measure fast-time responses of this system and use this measurements to identify slow-time damage states. Using this approach, PSW-based metrics are constructed to provide functional connection between measured fast-time dynamics and hidden slow damage accumulation. The SOD-base methods are applied to identify active damage states from the calculated PSW-based metrics.

3.1. The Old Procedure

To identify multi-dimensional damage, first step is to establish connection between measured fast-time time series and hidden damage states. The fast-time measurements, sampled at uniform time intervals t_s, are used to reconstruct an extended phase space trajectory of the system [24]. In delay coordinate embedding [21], measured scalar time series $\{x(r)\}_{r=1}^{M}$ are converted into a series of vectors $\{\mathbf{y}^T(r) = [x(r), x(r+\tau), \ldots, x(r+(d-1)\tau)] \in \mathbb{R}^d\}_{r=1}^{M-(d-1)\tau}$, where τ is a suitable time delay, and d is an appropriate embedding dimension. Both of these parameters can be determined using standard techniques [13, 17].

In the reconstructed phase space the state vectors are governed by some nonlinear map of the form

$$\mathbf{y}(r+1) = \mathbf{P}(\mathbf{y}(r); \phi), \tag{1}$$

where $\mathbf{P} : \mathbb{R}^d \to \mathbb{R}^d$. This map is parameterized by a damage variable ϕ since its evolution will cause distortions in the reconstructed phase space. In previous work [4], these changes in the vector field were described by a *PSW tracking function*

$$\mathcal{E}(\mathbf{y}; \phi) \equiv \mathbf{P}(\mathbf{y}; \phi) - \mathbf{P}(\mathbf{y}; \phi_0), \tag{2}$$

where Equation (2) ϕ_0 corresponds to a reference or healthy state of the damage variable.

For a given point $\mathbf{y}(r)$ on the reconstructed trajectory for a current damage state ϕ we do not need to evaluate $\mathbf{P}(\mathbf{y}; \phi)$ since $\mathbf{y}(r+1)$ is also available. However, we still need to know how this system *would have* evolved for the reference value of ϕ_0. As in the previous work, we use local linear modeling for this purpose:

$$\mathbf{y}(r+1) = \mathbf{A}_r \mathbf{y}(r) + \mathbf{a}_r, \tag{3}$$

where $\mathbf{A}_r$ is a $d \times d$ matrix and $\mathbf{a}_r$ is a $d \times 1$ vector. These local linear models are determined by calculating the best linear fit between N nearest neighbors of $\mathbf{y}(r)$ and their future states in a reference phase space where $\phi = \phi_0 + \mathcal{O}(\epsilon t_s)$. Note that, other modeling solutions may be more appropriate in practical applications.

Then an *estimated tracking function* for the initial point $\mathbf{y}(r)$ can be written as

$$\mathbf{E}(\mathbf{y}(r); \phi) = \mathbf{y}(r+1) - \mathbf{A}_r \mathbf{y}(r) - \mathbf{a}_r \tag{4}$$

and it can be determined experimentally. Use of $\mathbf{E}$ in place of $\mathcal{E}$ is justified, if local linear modeling errors are small compared to $\mathbf{E}$.

In previous work [5], average values of the estimated tracking function were evaluated in N_s disjoint regions $\mathcal{B}_i$ ($i = 1, \ldots, N_s$) of the reconstructed phase space

$$\mathbf{e}^i(\phi) = \|\mathcal{B}_i\|^{-1} \sum_{\mathbf{y} \in \mathcal{B}_i} \mathbf{E}(\mathbf{y}; \phi)\,, \tag{5}$$

and combined a *damage tracking feature vector*:

$$\mathbf{S} = [\mathbf{e}^1; \mathbf{e}^2; \ldots; \mathbf{e}^{N_s}]\,, \tag{6}$$

where $\mathbf{S}$ is a $dN_s \times 1$ vector calculated afresh for each data record.

The damage tracking feature vectors $\mathbf{S}$ are used directly to determine the observable facts about the hidden damage state. The mean is subtracted from the feature vectors and they are arranged in time sequence as columns of *tracking matrix* $\mathbf{Y}$. The damage identification is achieved by applying the SOD to this $\mathbf{Y}$. The SOD [7] is a generalization of the optimal tracking method [3] that relies on the existence of underlying deterministic behavior of the damage accumulation process but does not require its model. This method is based on maximizing smoothness and overall variation in the feature vectors, found by solving the following generalized eigenvalue problem:

$$[\mathbf{Y}^T\mathbf{Y}]\mathbf{q} = \lambda[(\mathbf{DY})^T\mathbf{DY}]\mathbf{q}\,. \tag{7}$$

where $\mathbf{D}$ is a differential operator [7]. The eigenvectors corresponding to the largest eigenvalues give the optimal eigenvectors $\mathbf{q}$ or *smooth orthogonal modes* (SOMs). Then $\boldsymbol{\varphi} = \mathbf{Yq}$ are *smooth orthogonal coordinates* that provide the linear projections of $\mathbf{Y}$, which have maximized smoothness and overall variation. As in previous work, in experiments, two main hypothesis will be tested:

Hypothesis # 1: the m largest eigenvalues of Equation (7) will be several magnitudes of order larger than the rest in the presence of m-dimensional damage evolution process.

Hypothesis # 2: the corresponded tracking modes will be within a linear transformation of the actual damage states.

3.2. New Damage Tracking Feature Vectors

In our original study, the reconstructed phase space was partitioned into uniform hypercuboids along the middle coordinate of the reconstructed $\mathbf{y}$ points. This procedure had two main objectives. Firstly, it was aimed at reducing fluctuations in the sensitivity to damage in partitions that was the source of noise in earlier studies; and secondly, it allowed for forming a multi-dimensional feature vector. This partitioning was shown to be adequate to reduce the the variance in the sensitivity to damage within one partition to yield convincing results. However, the remaining variance within one partition was still too high to provide robustness needed in practical applications.

Here, as an alternative, we use the equiprobable partition approach, where the phase space is partitioned with a condition that the number of points in each hypercuboid is the same. In this way we are assured that each partition will be more locally constrained and the points within are expected to have similar sensitivity to damage. In the new procedure following steps are used to section the reconstructed phase space:

Step 1: Cut the whole phase space into k disjointed hypercuboids along the first dimension (which is the same procedure as before).

Step 2: Divide each hypercuboid into k hypercuboids along the second dimension.

Step 3: Repeat *Step 2* with the next dimension until some preset p-th dimension ($p < d$).

In this way, the phase space is partitioned into $N_s = k^p$ disjoint hypercuboids.

A damage tracking matrix is constructed, as before, using the new feature vectors $\mathbf{S}$ which are estimated for N_r data records. These vectors are arranged in a $N_r \times d\, N_s$ matrix, called $\mathbf{Y}$.

4. Description of Experiment

To test the main hypotheses advanced in the previous section an experimental system is constructed to simulate a two-dimensional damage accumulation process. The experimental apparatus is based on a modified version of the well-known, two-well magneto-elastic oscillator described in [4]. The oscillator (see Figure 1) consists of a cantilever beam, which is constrained to one degree-of-freedom motion using stiffeners and is mounted on an electro-magnetic shaker. The nonlinear potential at the beam tip is realized by two permanent/electromagnet stacks, which are powered by a two-channel programable power supply. The supply voltages to the electromagnets are altered using a computer control of the power supply. Besides of an accelerometer, two laser vibrometers are used to measured the positions of the beam and the frame respectively (ch1 and ch2). The oscillation of the beam is recorded by differential output of the two vibrometers and the accelerometer. A shaker provides harmonic excitation to the mounting frame. The frequency and amplitude of the excitation are also computer controlled.

Data acquisition and control is conducted using a PC workstation equipped with a National Instruments PCI-6052E multi-channel data acquisition card and the LabView programming environment. This PC-based system is used to digitize and record signals from the laser vibrometers, and the power supply's terminal voltages. It is also used to provide a harmonic driving signal to the electromagnetic shaker. The programable power supply (Agilent E3647A) is controlled through RS-232 interface under the LabView instrumental control environment.

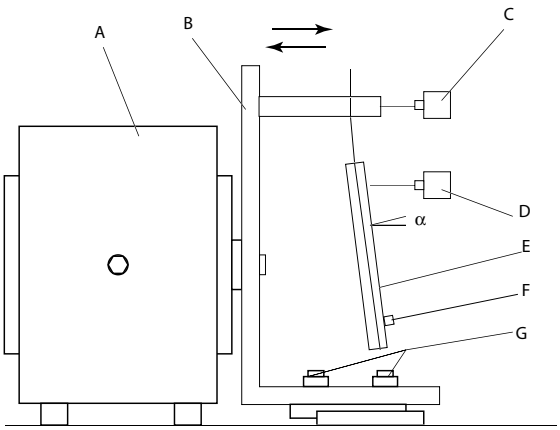

Figure 1. Experimental apparatus: (A) electromagnetic shaker, (B) sliding frame, (C) laser vibrometer ch1, (D) laser vibrometer ch2, (E) cantilever beam, (F) Accelerometer, and (G) permanent/electromagnet stacks.

For the experiment, the frame is forced with a 10 Hz harmonic signal. Amplitude of the driving signal is set to obtain nominally chaotic response for a fully loaded electromagnets. The voltage supplied to the electromagnets is altered harmonically according to the following equations:

$$v_1(t) = 9\cos(1.75 \times 10^{-4}t) + 10, \quad \text{and}$$
$$v_2(t) = 9\cos(3.5 \times 10^{-4}t - \pi/2) + 10\,.$$

Voltage updates are done for every 1.14 mV change in the amplitude. Refer to Figure 2 for the voltage time histories throughout the experiment. The frequency response functions (FRFs) of small oscillations in each energy well are estimated to quantify the overall influence of the change in the supply voltage on the parameters of fast-time system. Figure 3 shows the FRFs calculated for the minimum and maximum expected voltage supply for the electromagnets in the front and back energy wells. From corresponding data the maximum change in the natural frequency is calculated to be approximately 4%, which corresponds to the maximum 8% shift in the stiffness of the beam in each energy well.

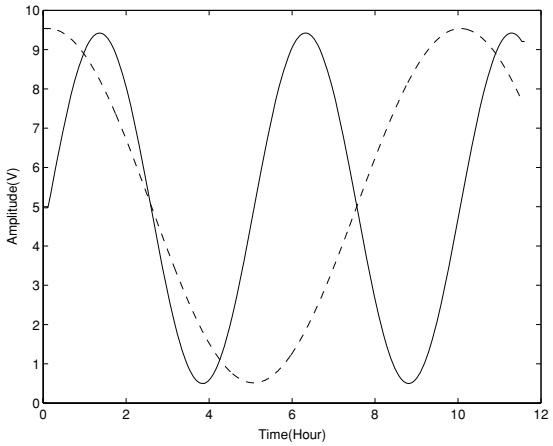

Figure 2. Voltage of the outputs of power supply. Solid line describes the voltage supplied to the front electromagnet, and dashed line to the back stack.

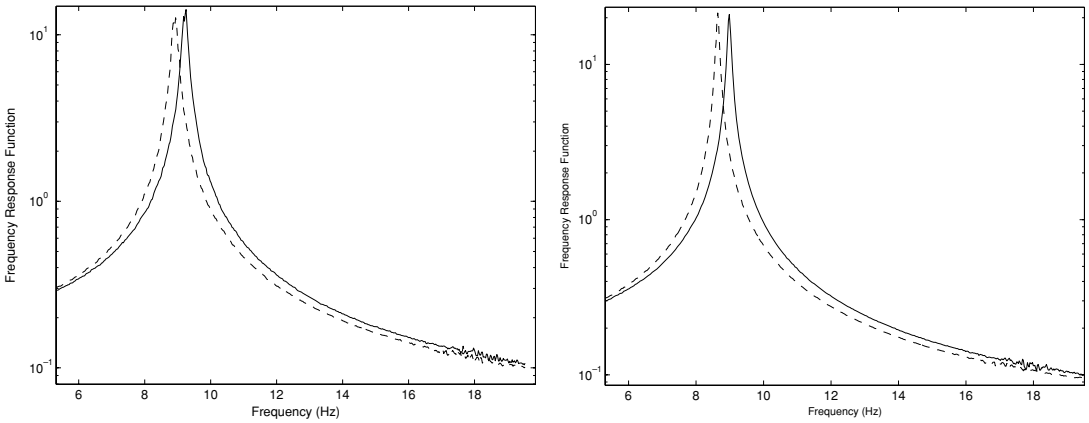

Figure 3. Frequency response functions for small oscillations in front (left plot) and back (right plot) energy wells. Solid line: 1 V on the stack and dashed line: 19 V on the stack.

During the experiments, the data from the laser vibrometers and the accelerometer are low-pass filtered with 50 Hz cutoff frequency, digitized with $1/t_s = 160$ Hz sampling frequency, and stored on a hard drive. The experiment lasts a little less than 12 hours, and a little over 6.6 million data points are recorded. During the experimental run, numerous bifurcations (transitions between a variety of observed apparently periodic and chaotic motions) in the system's response are observed.

The use of the laser vibrometers is motivated by the ability of running multiple experiments without altering the basic setup. They provide excellent repeatability and convenience. However, the quality of measurements is not as good as, for example, when strain gauges are used to measure the beam vibration [4, 6]. This is due to the sensitivity of the laser vibrometers to the change in lighting conditions, which is caused by different reflective properties of surfaces in front of the transducers. To minimize this effect during the experiments, an opaque shell is employed to cover the whole apparatus. In addition, a harmonic noise at the driving frequency is also introduced, which is due to the mismatch in the calibration of the transducers. However, this noise does not effect results of damage identification since it is stationary. Compared with data from the laser vibrometers, the data from the accelerometer includes more noise and are only used for comparison purposes. In the following sections, all data analysis results are based on the data from the laser vibrometers if it is not explicitly stated otherwise.

5. Damage Identification

The first 2^{15} points of the collected data are used to construct the reference local linear models. The delay time is estimated to be $6\,t_s$ and the embedding dimension of 5 is found to be sufficient to ensure unique embedding of the trajectories based on the measured scalar time series. The parameters of each linear model are estimated based on 32 nearest neighbors of each target point.

The differential time series (ch1-ch2) are divided into disjoint data records of $M = 2^{13}$ points in each. Based on this parameter, the collected data yields total of 800 data records of size M. To estimate the feature vectors $\mathbf{S}$ for each data record, the phase space is partitioned into $N_s = 81$ disjoint hypercuboids using $k = 3$ and $p = 4$ partitioning parameters. Time series corresponding to each coordinate of $\mathbf{S}$ are normalized and assembled into the matrix $\mathbf{Y}$ as described in the Section 3. For illustration purposes, several randomly chosen rows of $\mathbf{Y}$ are depicted in Figure 4.

The SOD-based damage identification is applied to the matrix $\mathbf{Y}$ and the resulting 20 largest generalized eigenvalues of Equation (7) are depicted in the left plot of Figure 5. First two largest generalized eigenvalues are clearly separated from the rest. In fact, this separation is very similar to the one reported in our previous work [5] using simulated data. The relative prominence of the third and the forth largest generalized eigenvalues can be explained by the presence of experimental noise.

Please note that it is usually customary to use at least 10,000 points per each dimension to accurately estimate statistics from a chaotic data. In our case, since the embedding dimension was $d = 5$, this requirement would result into 50,000 points. In our calculations, we have only used approximately 100 points for estimating each $\mathbf{e}$ and 2^{13} points for each $\mathbf{S}$. This is about two and one order of magnitude deficiency, respectively, in the available amount of data. Even with this limited amount of data we still have indication that there are two main independent factors contributing to the smooth variations in the tracking matrix $\mathbf{Y}$. Thus, first hypothesis about the separation of eigenvalues is validated experimentally.

In the right plot of Figure 5 generalized eigenvectors or *smooth orthogonal coordinates* (SOCs) corresponding to the two largest generalized eigenvalues from Figure 5 are shown. From this figure, it is clear that the second SOC has considerably larger local fluctuations compared with the first SOC, which is in correspondence with the magnitude difference between the second and first largest eigenvalues.

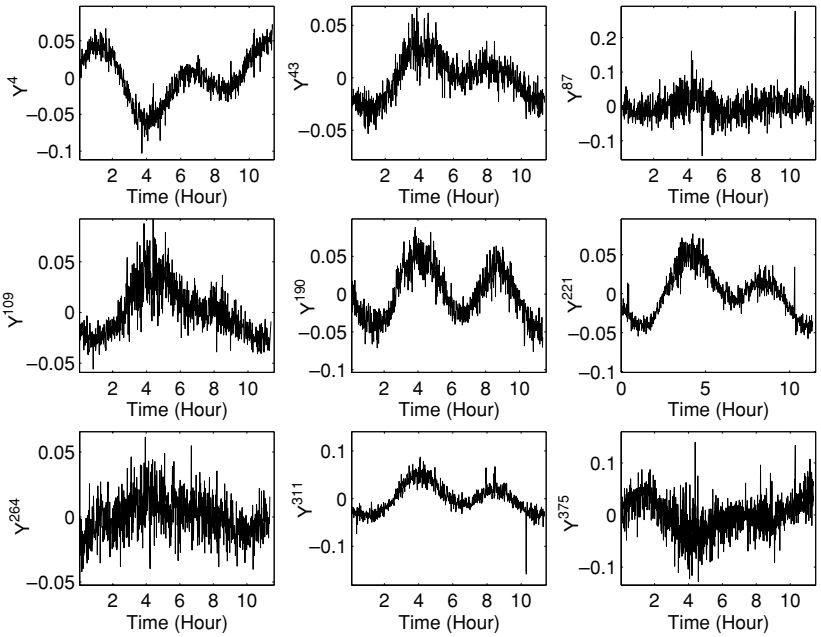

Figure 4. Sample of randomly chosen columns of the tracking matrix $\mathbf{Y}$.

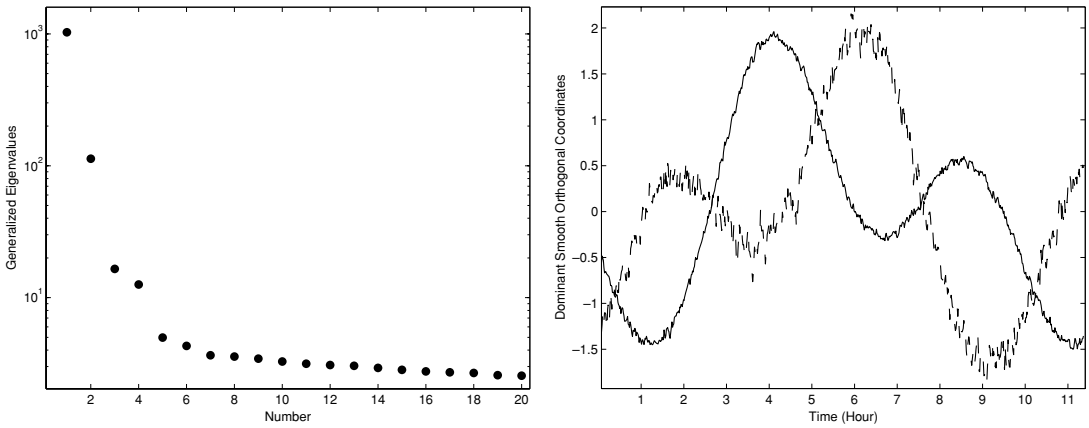

Figure 5. Left plot: first 20 largest generalized eigenvalues of Equation (7) for a base experiment. Right plot: the SOCs identified from the time series. Solid line shows tracking modes corresponding to the largest eigenvalue, and dashed line corresponds to the second largest eigenvalue.

The first indication that our second hypothesis is valid is depicted in the left plot of the Figure 6. Here the first and second SOCs are compared to a linear combination of actual damage states (power supply terminal voltages). We have plotted $v_1 + v_2$ and $v_1 - v_2$ on top of scaled the SOCs in Figure 6. Clear similarity between them is observed. This relationship was expected from the definition of the SOD since the maximum variances in the voltage phase space are observed for $v_1 = \pm v_2$ directions. To further investigate the validity of hypothesis # 2 the phase space trajectory of damage is compared with the identified phase space trajectory scaled according to the parameters found for Figure 6 in least squares sense. The results are shown in the right plot of Figure 6. It is clear that these trajectories are

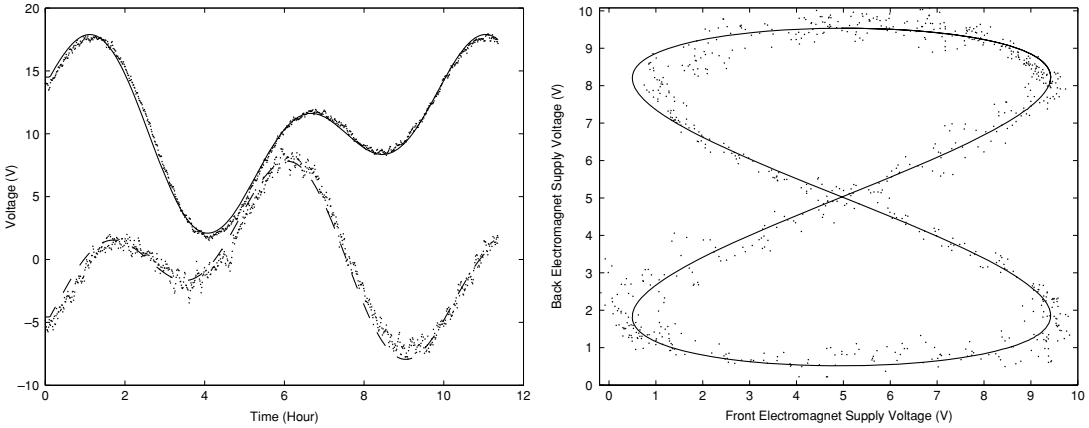

Figure 6. Left plot: two combinations of the two input voltages ($v_1 + v_2$ solid line and $v_1 - v_2$ dashed line), and the scaled first two SOCs (dots). Right plot: phase trajectory of the power supply terminal voltage (solid line) and the identified trajectory after affine transformation (dots).

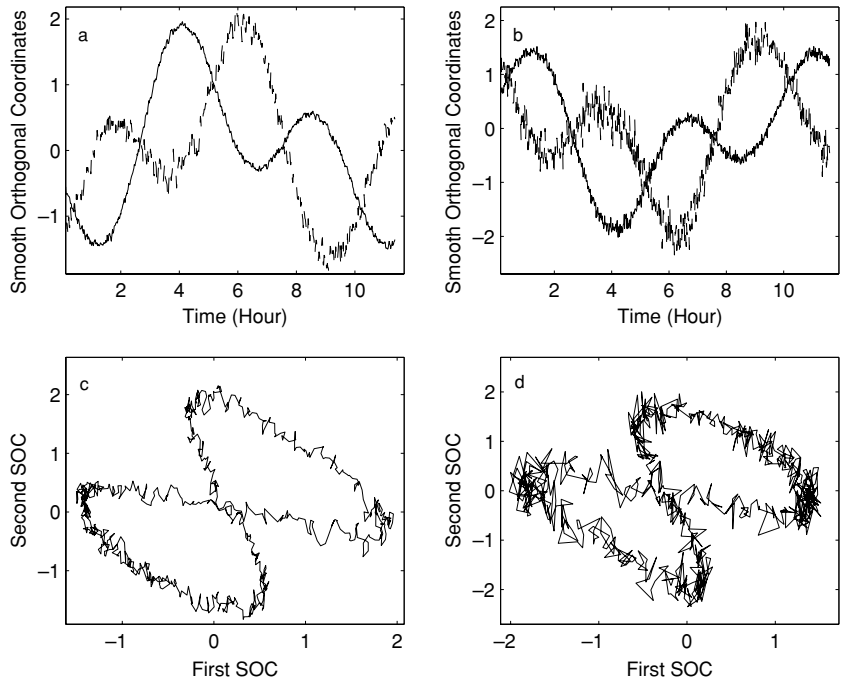

Figure 7. Plot of the SOCs base on the new partition method (a) and the original partition method (b). Corresponding phase portrait plots (c) and (d), respectively.

not only qualitatively similar, but there exists a one-to-one affine map that maps the identified damage phase trajectory to the actual damage trajectory.

Figure 7 is used to demonstrate the improvement in the quality of the tracking caused by the new partition method. The SOCs and their phase portrait based on the new partitioning method are depicted in Figure 7(a) and (c), respectively. Corresponding plots for the original method, where the reconstructed phase space is partitioned into 16 unform sections, are shown in Figure 7(b) and (d). It is clear that the

Table 1. Quality of the identified SOCs versus the data record size.

Experiment	Data record size	SNR (dB)
1	2^{12}	16.541
2	2^{13}	17.226
3	2^{14}	22.595

tracking modes and phase portrait for the new partition method have much smaller local fluctuation. In fact this improvement results into a two dB increase in the signal-to-noise ration (SNR) from 15.226 dB to 17.226 dB.

To illustrate the effect of the data record size on the quality of tracking, another two experiments are conducted. In the new experiments the size of the data record is altered by a factor of two resulting in $M = 2^{12}$ and $M = 2^{14}$ points. Output functions of the power supply are changed accordingly to keep rate of damage evolution constant in the corresponding data records for each experiment. Table 1 shows the SNRs for the identified SOCs in all three experiments. It is apparent that the increase in the data record size provides considerable improvement in the quality of the identified SOCs.

Data from accelerometer were also analyzed using same steps as introduced above, and corresponding identification results are shown in Figure 8. The identification results can also be used to validate our two main hypotheses, and it is obvious that our method does not depend on any specific choice of sensing device or measurement point.

6. Conclusion

In this paper, we have presented an experimental confirmation of a multi-dimensional damage identification procedure that was reported in [5]. In addition, a new phase space partitioning scheme was proposed that significantly improved the identification results. The experiment was designed to introduce a two-dimensional slow-time damage process into a fast-time dynamical system of a one degree-of-freedom

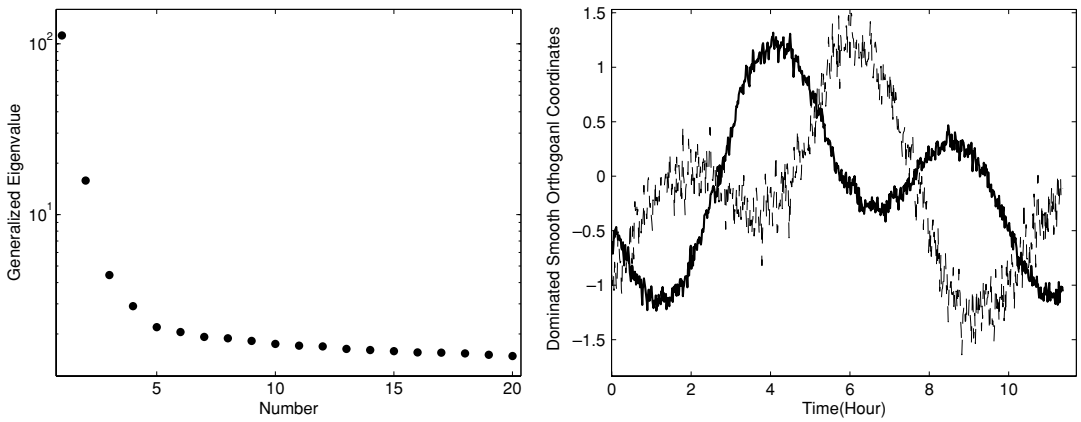

Figure 8. Left plot: first 20 largest generalized eigenvalues using the data collected from the accelerometer. Right plot: the SOCs identified using the data collected from the accelerometer. Solid line shows tracking modes corresponding to the largest eigenvalue, and dashed line corresponds to the second largest eigenvalue.

driven oscillator. The system was a modified version of the two-well magneto-elastic oscillator as studied in [4]. The slow-time damage accumulation was introduced by powered electromagnets that perturbed the potential field of a vibrating cantilever beam. The effect of this perturbation was a maximum of 8% change in the stiffness of the beam in each potential well.

The beam vibration was recorded using the laser vibrometers and the accelerometer. The original damage identification scheme was modified by a new phase space partitioning method that was shown to considerably improve the quality of the identified SOCs. It was shown that in experimental procedure, the SOD-based damage identification scheme is still able to identify a two-dimensional damage process. The corresponding SOCs were shown to be in approximately linear, one-to-one correspondence with the actual damage states that were measured independently. Namely, it was demonstrated that the identified battery voltage phase space trajectories are in an affine relationship with the original control trajectories. The improvement in the quality of the experimentally identified SOCs with the increase in the available data was also demonstrated. In addition, the analysis based on data recorded from both laser vibrometers and accelerometer showed that the proposed method does not depend on any specific choice of a sensing device.

Acknowledgments

This paper is based upon work supported by the National Science Foundation under Grant No. 0237792.

References

1. Adams, D. E. and Nataraju, M., 'A nonlinear dyanamical systems framework for structural diagnosis and prognosis', *International Journal of Engineering Science* **40**, 2002, 1919–1941.
2. Bachschmid, N., Pennacchi, P., and Vanai A., 'Identification of multiple faults in rotor systems', *Journal of Sound and Vibration* **254**(2), 2002, 327–367.
3. Chatterjee, A., Cusumano, J. P., and Chelidze, D., 'Optimal tracking of parameter drift in a chaotic system: Experiment and theory', *Journal of Sound and Vibration* **250**(5), 2002, 877–901.
4. Chelidze, D., Cusumano, J., and Chatterjee, A., 'Dynamical systems approach to damage evalution tracking, part i: Desccription and experimental application', *Journal of Vibration and Acoustics* **124**(2), 2002, 250–257.
5. Chelidze, D., 'Identifying multidimensional damage in a hierarchical dynamical system', *Nonlinear Dynamics* **37**, 2004, 307–322.
6. Chelidze, D. and Cusumano, J. P., 'A dynamical system approach to failure prognosis', *Journal of Vibration and Acoustics* **126**, 2004, 2–8.
7. Chelidze, D. and Liu, M., 'Dynamical systems approach to fatigue damage identification', *Journal of Sound and Vibration* **281**(3–5), 2005, 877–904.
8. Cusumano, J. P. and Chatterjee, A., 'Steps towards a qualitative dynamics of damage evolution', *International Journal of Solids and Structures* **37**(44), 2000, 6397–6417.
9. Cusumano, J., Chelidze, D., and Chatterjee, A., 'Dynamical systems approach to damage evalution tracking, part ii: Model-based validation and physical interpretation', *Journal of Vibration and Acoustics* **124**(2), 2002, 258–264.
10. Doebling, A. W., Farrar, C. R., Prime, M. B., and Shevitz, D. W., Damage identification and health monitoring of structural and mechanical systems from changes in their vibration characteristics: A literature review, Tech. Rep. LA-13070-MS, Los Alamos National Laboratory, Los Almos, NM, 1996.
11. Doebling, S., Farrar, C. R., and B., P. M., 'A summery review of vibrastion-based damage identification methods', *Shock and Vibration Digest* **30**, 1998, 91–105.
12. Edwards, S., Lees, A. W., and Friswell, M. I., 'Fault diagnosis of rotating machinery', *Shock and Vibration Digest* **30**(1), 1998, 4–13.
13. Fraser, A. and Swinney, H., 'Independent coordinates for strange attractors from mutual information', *Physical Review A* **33**(2), 1986, 1134–1140.

14. Foong, C.-H., Pavlovskaia, E., Wiercigroch, M., and Deans, W. F., 'Chaos caused by fatigue crack growth', *Chaos, Solitons and Fractals* **16**, 2003, 651–659.
15. Gorl, E. and Link, M., 'Damage identification using change of eigenfrequencies and mode shapes', *Mechanical Systems and Signal Processing* **17**(1), 2003, 103–110.
16. Hively, L. M. and Protopopescu, V. A., 'Machine failure forewarning via phase-space dissimilarity measures', *Chaos* **14**(2), 2004, 408–419.
17. Kennel, M. B., Brown, R., and Abarbanel, H., 'Determining embedding dimension for phase-space reconstruction using a geometric construction', *Physical Review A* **45**(6), 1992, 3403–3411.
18. Linderholt, A. and Abrahamon, T., 'Parameter identifiability in finite element model error localisation', *Mechanical Systems and Signal Processing* **17**(3), 2003, 579–588.
19. Nichols, J. M., Todd, M. D., Seaver, M., and Virgin, L. N., 'Use of chaotic excitation and attractor property analysis in structural health monitoring', *Physical Review E* **67**, 2003, (016209).
20. Nichols, J. M., Trickey, S. T., Todd, M. D., and Virgin, L. N. 'Structural health monitoring through chaotic interrogation', *Meccanica* **38**, 2003, 239–250.
21. Sauer, T., Yorke, J. A., and Casdagli, M., 'Embedology', *Journal of Statistical Physics* **65**(3-4), 1991, 579–616.
22. Sinha, J. K., Friswell, M. I., and Edwards, S., 'Simplified models for the location of cracks in beam structures using measured vibration data', *Journal of Sound and Vibration* **251**(1), 2002, 13–38.
23. Sohn, H., Farrar, C. R., Hemez, F. M., Shunk, D. D., Stinemates, D. W., and Nadler, B. R., A review of structural health monitoring literature: 1996–2001, Tech. Rep. LA-13976-MS, 2003, Los Alamos National Laboratory, Los Almos, NM, 2003.
24. Takens, F., 'Detecting strange attractor in turbulence', in *Dynamical Systems and Turbulence, Warwick*, D. A. Rand and L. S. Young (eds). Springer Lecture Notes in Mathematics, Springer-Verlag, Berlin, 1981, pp. 336–381.
25. Todd, M. D., Nichols, J. M., Pecora, L. M. and Virgin, L. N., 'Vibration-based damage assessment utilizing state space geometry changes: local attractor variance ratio', *Smart Materials and Structures* **10**, 2001, 1000–1008.
26. Todd, M. D., Erickson, K., Chang, L., Lee, K., and Nichols, J. M., 'Using chaotic interrogation and attractor nonlinear cross-prediction error to detect fastener preload loss in an aluminum frame', *Chaos* **14**(2), 2004, 387–399.
27. Wang, W. J., Chen, J., Wu, X. K., and Wu, Z. T., 'The application of some nonlinear methods in rotating machinery fault diagnosis', *Mechanical Systems and Signal Processing* **15**(4), 2001, 697–705.
28. Zhou, G. and Sim, L. M., 'Damage detection and assessment in fibre-reinforced composite structures with embedded fibre optic sensors-review', *Smart Materials and Structures* **11**, 2002, 925–939.
29. Zou, Y., Tongand, L., and Steven, G. P., 'Vibration-based model-dependent damage (delamination) identification and health monitoring for composite structures – a review', *Journal of Sound and Vibration* **230**(2), 2000, 357–378.